



Article

Assessment of Influential Operational Parameters in the Mitigation of CO₂ Emissions in a Power Plant: Case Study in Portugal

Vítor Balanuta ¹, Patrícia Baptista ² , Fernando Carreira ³, Gonçalo O. Duarte ^{2,4} and Cláudia S.S.L. Casaca ^{4,*} 

¹ ISEL—Instituto Superior de Engenharia de Lisboa, Polytechnic University of Lisbon, 1959-007 Lisboa, Portugal; a48448@alunos.isel.pt

² IN+, Center for Innovation, Technology and Policy Research—Instituto Superior Técnico, Universidade de Lisboa, 1049-001 Lisboa, Portugal

³ UniRE, ISEL—Instituto Superior de Engenharia de Lisboa, Polytechnic University of Lisbon, 1959-007 Lisboa, Portugal

⁴ CIMOSM, ISEL—Instituto Superior de Engenharia de Lisboa, Polytechnic University of Lisbon, 1959-007 Lisboa, Portugal

* Correspondence: claudia.casaca@isel.pt

Abstract: The European decarbonization goals and requirement for energy independence are mostly relying on intermittent renewable energy sources for electrification. A numerical model was developed to simulate the operation of a steam generator, allowing a study of the potential impacts of retrofitting existing coal-fired power plants to operate with biomass or coal–biomass mixtures on combustion parameters and CO₂ emissions. The results obtained using the operational parameters of the Sines power plant indicate that a mixture of 25% coal and 75% pine sawdust allow operation at $\lambda = 1.8$, demonstrating that a small amount of coal allows operation near the coal combustion parameters ($\lambda = 1.9$). These conditions have the drawback of a reduction of 8.7% in adiabatic flame temperature but a significant reduction of 57.5% in CO₂ emissions, considering the biomass as carbon-neutral.

Keywords: greenhouse gas emissions; biomass; thermal power plant; retrofitting; decarbonization



Citation: Balanuta, V.; Baptista, P.; Carreira, F.; Duarte, G.O.; Casaca, C.S.S.L. Assessment of Influential Operational Parameters in the Mitigation of CO₂ Emissions in a Power Plant: Case Study in Portugal. *Clean Technol.* **2024**, *6*, 1169–1180. <https://doi.org/10.3390/cleantechnol6030057>

Academic Editor: Dmitry Yu. Murzin

Received: 18 July 2024

Revised: 28 August 2024

Accepted: 2 September 2024

Published: 6 September 2024



Copyright: © 2024 by the authors. Licensee MDPI, Basel, Switzerland. This article is an open access article distributed under the terms and conditions of the Creative Commons Attribution (CC BY) license (<https://creativecommons.org/licenses/by/4.0/>).

1. Introduction

Greenhouse gas (GHG) emissions must be reduced on a global scale. Regarding the European Union, the progressive reduction in the import of Russian fossil fuels, particularly in central European countries, has accelerated the transition toward the elimination of fossil fuels. This applies across various sectors, including transportation, buildings, manufacturing, and energy [1]. The European Union (EU) has set the goal of leading by example in deploying renewable energy as well as transforming energy and transportation infrastructure to promote a fast transition to electrification [2,3].

In the Portuguese context, according to the National Energy and Climate Plan (PNEC) [4], intensive measures to reduce GHG emissions must be implemented until 2030, which are also articulated with the Roadmap for Carbon Neutrality (RNC) [5]. The sectors with high energy consumption typically rely on nonrenewable sources, and thus a transition to electricity has been identified as a crucial measure for mitigating greenhouse gas emissions. The target is that electricity produced exclusively from renewable sources will represent 65% of Portugal's final energy consumption by 2050 [6,7]. However, the energy increase associated with this transition, in conjunction with the intermittency of renewables, may present challenges to the implementation of the PNEC and RNC.

Moreover, the external energy dependence in Portugal, particularly in the context of electricity imports and fossil fuels (including electricity production), makes the country

vulnerable to foreign policy and the market fluctuations associated with these fuels. Therefore, it is urgent to implement improvements in the efficiency of nonintermittent electricity production systems. Thermal power plants play a pivotal role in this context, having the potential to reduce fossil fuel consumption, diversify fuel sources, minimize greenhouse gas emissions, and contribute to the pursuit of environmental sustainability goals.

The growing emphasis on renewable energies sources in Portugal is evidenced by a reduction in energy dependence by approximately 9 p.p. between 2015 and 2021. Nevertheless, energy dependence remains relatively high (approximately 67% in 2021), having associated economic and environmental costs. Additionally, the percentage of electricity produced from dedicated and cogeneration powerplants in 2021 largely relied on natural gas imported from the United States and Algeria [8].

Historically, in Portugal, the production of electricity using natural gas has effectively contributed to the decarbonization process, when electrification accounted for at least one-third of the total exergy consumed. Furthermore, renewable energy sources represented over one-third of the energy mix, and natural gas imports constituted at least one-third of the fossil fuel mix used for electricity generation [6].

In order to meet the anticipated growth in electricity demand, it is essential to enhance the capacity of the production system and diversify the supply, while also expanding the energy provided by renewable sources. This will ensure that national and European decarbonization goals are achieved. It is, however, of utmost importance to guarantee that the intermittency of renewable energy production does not coincide with peak consumption periods. Alternatively, reinforcing the output of existing thermal power plants by improving efficiency or utilizing different fuels (with lower carbon intensity or from renewable sources) may prove to be a viable solution [9].

The diversification of energy sources is increasingly important within the current global context. Currently, Portugal faces commercial price fluctuations, particularly for oil and natural gas, resulting from economic and/or political crises. This context has been particularly relevant regarding the import of fossil energy sources from Russia and from countries on which Portugal had a high level of dependence, which has resulted in compromised energy security and a reduction in green technology innovation [10]. Before 2022 year, Europe imported approximately 40% of its natural gas, 23% of its oil, and 47% of its coal from Russia [11]. A European-level analysis indicated that countries with low reliance on Russian natural gas (such as Portugal) have a positive relationship with green innovation when natural gas imports are involved. However, for countries heavily dependent on Russian gas, the opposite effect was observed [10].

For instance, Germany, the Czech Republic, and Finland have witnessed an uptick in coal utilization for electricity generation [12], resulting in elevated CO₂ emissions. It is therefore evident that there is a need to diversify energy sources and to consider the potential of coal-fired power plants to balance the grid, particularly if they are included in a decarbonization plan. The prospective implementation of carbon emission quotas and related costs may exert a considerable impact on the design of electricity production systems. In particular, the implementation of a system of quotas and CO₂-related costs in existing coal-fired power plants could facilitate the adoption of retrofitting solutions for coal and biomass co-combustion [13]. At the local level, the prices of biomass (which may be subsidized), coal, and CO₂ will play a pivotal role in the decision-making process for retrofitting existing coal-fired plants [13]. Implementing optimization in the steam generators of decommissioned power plants may also stimulate the national market to use biomass, while preserving historical investments in coal-fired facilities.

In Portugal, there has been a significant decline in national coal imports, with a reduction of 99.7% compared to 2015 levels. This reduction can be attributed to the decreased utilization of power plants that employ this technology, as part of the national decarbonization strategy [8]. The three coal-fed thermal power plants deactivated in recent years generated about 2000 MW of electricity. Between 2016 and 2019, this accounted for about 39% of the thermally generated electricity in Portugal [8]. Consequently, there

has been an increase in energy production through photovoltaic systems and energy imports from the European grid to compensate for this reduction in coal-fired electricity generation [8]. However, this energy dependence has become increasingly important after coal-fired power plants were decommissioned: between 2016 and 2018 Portugal was able to export a total of 10,426 GWh of electricity and between 2019 and 2021, Portugal had to import a total of 9608 GWh [8].

Between 2016 and 2022, the electricity produced from biomass averaged 12.5% of the total. The combustion of plant and forest residues, sulfite liquors, biogas, and municipal solid waste (renewable portion) represents a means of limiting emitted carbon due to the consideration of the carbon cycle [8]. Furthermore, the co-combustion of coal and biomass allows for the reduction in greenhouse pollutants such as carbon dioxide (CO₂), sulfur dioxide (SO₂), and nitrogen oxides (NO_x) at a low investment cost [14].

The co-combustion of coal and biomass offers several advantages regarding lowering ignition temperature and reducing CO₂ emissions, with biomass potentially being considered carbon-neutral or even carbon-negative in emission accounting. However, the lower calorific value of biomass results in lower flame temperatures [15].

In the context of a thermal power plant, the steam generator represents a major component of the system, as it serves to interconnect the combustion process with the production of steam. This component plays a pivotal role in defining the operational parameters of the thermodynamic cycle, including working pressures and respective temperatures, as well as the transfer of heat released from fuel combustion to the water-steam circuit [16].

Due to the complexity of using various types of fuel or even co-combustion and its interconnection with the thermodynamic water-steam cycle, numerical simulation may be relevant for determining which operating conditions of the thermodynamic cycle and the associated combustion parameters can be further adjusted. As an example, numerical tools showed that biomass can contribute to a 6% reduction in GHG emissions through the replacement of 3.8% of the coal currently employed [17]. Likewise, the co-combustion of coal and biomass was demonstrated to facilitate a reduction in carbon emissions by up to 25% [18]. Consequently, numerical tools can be employed to facilitate the preliminary design and evaluation of operational parameters, alongside the assessment of associated energy and environmental impacts [15].

The objective of this work was to perform a preliminary analysis of the steam generator of a 176 MW coal-fired power plant, with the goal of evaluating influential operational parameters that could be employed to mitigate CO₂ emissions by using biomass. Coal, pine sawdust, and several mixtures of both fuels were tested with excess air coefficients of between 1 and 2.2; the resulting CO₂ emissions, adiabatic flame temperature, and energy transferred to the steam generator heat exchangers were evaluated. For our purpose, a numerical model was developed to simulate the operation of a steam generator that is able to be used to test different fuels and operational conditions to evaluate the production of electricity, considering the impact on GHG emissions, based on established decarbonization goals.

2. Methodology

Water-tube boilers are the most prevalent configuration for steam generators in the context of thermal power plant applications. These generators are designed to operate at high pressures and produce substantial thermal energy [19]. The operational principle of a steam generation apparatus is primarily based on the utilization of high-temperature exhaust gases generated by fuel combustion, moving within the generator due to the existence of pressure and temperature gradients. This enables the transfer of heat to the water within the heat exchangers.

Figure 1 illustrates the heat exchanges within a steam generator, namely, for the economizer, vaporization panels, reheater and superheater. This diagram includes the rationale implemented in the numerical model we developed to simulate a steam generator

for the thermodynamic analysis of the water–steam circuit in points 1 to 6 (Section 2.1) and the heat exchange (represented by H) in the air–fume circuit (Section 2.2). The simulation tool was developed in Python.

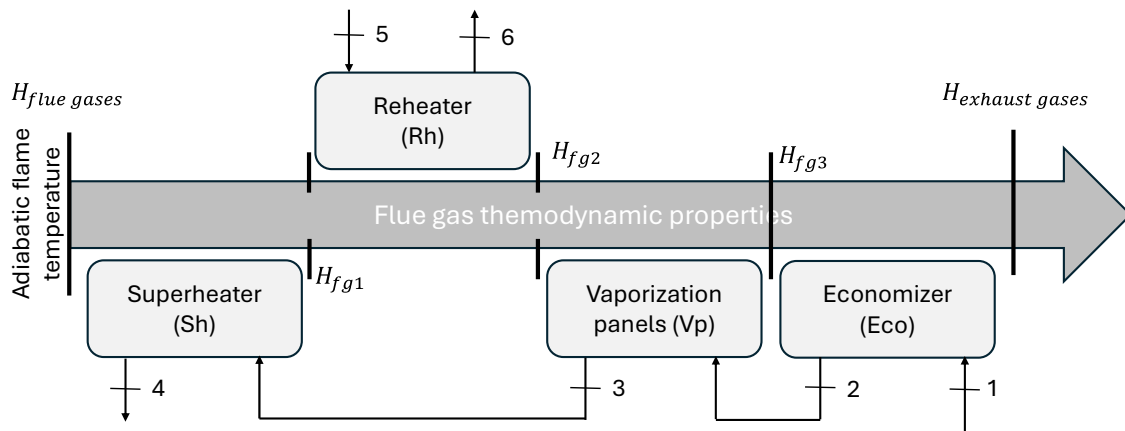


Figure 1. Schematic of the heat transfer in a steam generator.

2.1. Water–Steam Circuit

Water is introduced into a steam generator through an economizer, which is heated (in compressed liquid state) by energy transfer of low-temperature flue gases (between 350 °C and 400 °C) [20]. The temperatures of the water inlet and outlet are contingent upon the operating pressure of the steam generator [21]. In addition to the properties of the materials utilized in the economizer, the approach point represents a crucial parameter in the economizer design. This parameter indicates the difference between the saturation temperature imposed on the vaporization panels and the temperature of the water at the economizer outlet. It is recommended in the literature that the temperature of the water exiting the economizer be between 10 and 15 °C lower than the saturation temperature [22].

Vaporization panels are partially included in the walls of the steam generator, which are where the water phase change takes place. The latent heat associated with this transformation is considered specifically for the vaporization panels.

Superheaters are indispensable components in the steam boilers utilized in power plants and other industrial processes, being essential in raising the temperature of the steam generated. However, their operation is constrained by specific metallurgical limitations, predominantly due to the elevated temperatures and pressures involved [23].

The superheater's operating conditions are contingent upon the nominal operating pressure of the steam generator, aiming to maintain steam temperatures typically around 570 °C. Usually, the reheater operates at one-quarter of the operating pressure and at similar temperatures to those at the superheater outlet [24].

The circuit implemented in this work consisted of two steam heating stages: the main stage and the reheating stage. The working pressure was imposed along the steam generator and remained constant in the economizer, vaporization panels, and superheater. By default, the reheating stage operated at a quarter of the working pressure. Irreversibility, such as load loss, was not considered in the exchangers.

Our case study is based on the Sines thermal power plant, located in Portugal. The water–steam points (Figure 1) were calculated in accordance with the properties presented in Table 1.

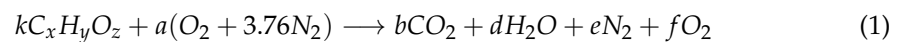
It should be noted that the irreversibility in the steam turbine, which occurs between points 4 and 5 (outlet of superheater and inlet of reheater, respectively), was not considered in this work. The ΔT defined in point 2 represents the temperature differential requisite for the economizer to operate exclusively with liquid water, being considered in this study a value of $\Delta T = 10$ °C, which is a typical value for the approach point (value within data from the literature).

Table 1. Operational conditions and thermodynamic properties of Sines power plant water–steam circuit.

Point	Pressure [MPa]	T [°C]	h [kJ/kg]	s [kJ/kg·K]
1	12.5	146	h ₁	s ₁
2	12.5	T _{sat} – ΔT	h ₂	s ₂
3	12.5	T _{sat}	h _{sat}	s _{sat}
4	12.5	567	h ₄	s ₄
5	1.6–6.3	T ₅	h ₅	s ₄ = s ₅
6	1.6–6.3	550	h ₆	s ₆

2.2. Air–Fumes Circuit

The combustion process is of paramount importance in thermal power plants, as it is the primary mechanism responsible for the formation of the combustion gases that traverse the air–fumes circuit. The excess air coefficient (λ) allows evaluating the air/fuel ratio of a given reaction in relation to its stoichiometric value. Typical coal-fired power plants operate with an excess air coefficient of 1.1. to 1.5, depending on combustion mode and coal characteristics [20]. This is also valid independent of the power plant load requirements [25]. The combustion reaction with excess air includes the presence of oxygen, O₂, in the flue gases (Equation (1)).



The fuel flow, \dot{m}_{comb} (in kg/s), to be supplied to the steam generator (Equation (2)) was calculated using the efficiency and useful power of the Sines plant (176 MW). The efficiency of the power plant was 30%.

$$\dot{m}_{comb} = \frac{\dot{W}_{useful}}{PCI \times \eta_{powerplant}} \quad (2)$$

The air flow (in kg/s) was determined by employing the stoichiometric air/fuel ratio, AFR_{st} , and the excess air coefficient (Equation (3)).

$$\dot{m}_{air} = \lambda \times AFR_{st} \times \dot{m}_{comb} \quad (3)$$

As λ is a variable parameter, dependent on the analysis performed, the moles of excess air in the reactants can be calculated using the known moles of fuel, k , following Equation (4).

$$a = \frac{k \times 1 \times AFR_{st} \times (xM_C + yM_H + zM_O)}{(M_{O_2} + 3.76M_{N_2})} \quad (4)$$

Once the moles of air and fuel were determined, the remaining moles of the reaction products were calculated using chemical species balances.

The adiabatic flame temperature (T_{ad}) was obtained by iteratively solving Equation (5). In this process, it was assumed that there was no dissociation and that the products obtained were only those presented in Equation (1). The standard enthalpy of combustion, ΔH_R° , is directly associated with the lower calorific value of fuel, LHV (kJ/kg) and the respective number of moles k .

$$\Delta H = \Delta H_R^\circ + \sum_{Products} n_i [\bar{h}(T_{ad}) - \bar{h}(T_{ref})] - \sum_{Reagents} n_j [\bar{h}(T) - \bar{h}(T_{ref})] = 0 \quad (5)$$

$$\Delta H_R^\circ = -LHV \times M_{fuel} \times k$$

For the sake of simplicity, it was assumed that the reactants were at the reference temperature, 298 K. The adiabatic flame temperature is directly dependent on the excess air coefficient and the type of fuel used. Table 2 contains typical values of the adiabatic flame temperature for three different fuels with different amounts of excess air.

Table 2. Typical values of adiabatic flame temperature and excess air for biomass, coal, and natural gas.

Parameter	Biomass	Coal	Natural Gas
Adiabatic flame temperature [K]	1073–2050 [26]	2224–2330 [25,26]	1050–2191 [26,27]
λ	1.2–6 [28–30]	1.1–3 [20,25,31]	1.05–5.5 [27,32,33]

The heat released by combustion is determined using the number of moles of fuel, k , required to fulfil the useful power demands of the plant and the excess air during the combustion (λ). This is calculated assuming the maximum temperature (adiabatic flame temperature) obtained from Equation (5). Equation (6) computes the correspondent absolute enthalpy ($\dot{H}_{flue\ gases}$) that can be transferred to the heat exchangers.

$$\dot{H}_{flue\ gases} = b_{CO_2} \times \bar{h}_{CO_2}(T_{ad}) + d_{H_2O} \times \bar{h}_{H_2O}(T_{ad}) + f_{O_2} \times \bar{h}_{O_2}(T_{ad}) + e_{N_2} \times \bar{h}_{N_2}(T_{ad}) \quad (6)$$

The energy available from flue gases is transferred to the heat exchangers. The required heat transfer in all the heat exchangers, \dot{Q}_{in} (kW), within the steam generator was obtained from a steam generator efficiency, $\eta_{generator}$, of 90% and the LHV of the fuel used, as shown in Equation (7).

$$\dot{Q}_{in} = LHV \times \dot{m}_{fuel} \times \eta_{generator} \quad (7)$$

In all heat exchangers, it was considered that the same mass flow of steam circulated. The determination of this quantity is contingent upon a comprehensive analysis of the enthalpy variation between the exit and entry conditions of each heat exchanger and the total heat transferred for the heat exchangers, \dot{Q}_{in} , which results from Equation (8).

$$\dot{m}_{steam} = \frac{\dot{Q}_{in}}{(h_4 - h_1) + (h_6 - h_5)} \quad (8)$$

The heat rate, \dot{Q} (kW), transferred to the heat exchangers is determined through the difference in enthalpies between the entry and exit of each exchanger (Equation (9)) and the known steam flow rate, \dot{m}_{steam} (kg/s), following the diagram presented in Figure 1.

$$\begin{aligned} \dot{Q}_{Eco} &= \dot{m}_{steam} \times (h_2 - h_1) \\ \dot{Q}_{Vp} &= \dot{m}_{steam} \times (h_3 - h_2) \\ \dot{Q}_{Sh} &= \dot{m}_{steam} \times (h_4 - h_3) \\ \dot{Q}_{Rh} &= \dot{m}_{steam} \times (h_6 - h_5) \end{aligned} \quad (9)$$

The interconnection between the water–steam and air–fume circuits occurs in the heat exchangers. For this analysis, it was assumed that the conditions governing the water entry and exit conditions in each exchanger were fixed, allowing the power plant to operate according to its original specifications. The sequence of heat exchanges that occur in the air–fume circuit is described in Equation (10), according to Figure 1.

$$\begin{aligned} \dot{H}_{fg1} &= \dot{H}_{flue\ gases} - \dot{Q}_{Sh} \\ \dot{H}_{fg2} &= \dot{H}_{fg1} - \dot{Q}_{Rh} \\ \dot{H}_{fg3} &= \dot{H}_{fg2} - \dot{Q}_{Vp} \\ \dot{H}_{exhaust\ gases} &= \dot{H}_{fg3} - \dot{Q}_{Eco} \end{aligned} \quad (10)$$

Once the parameters of the water–steam and the air–fume circuits were defined, it was possible to simulate different operating conditions for the steam generator regarding

the reheating operating pressures and the influence of the properties of the fuel and its combustion parameters on heat transfer.

2.3. Definition of Scenarios

The case study scenarios involved the operating conditions of the Sines thermal power plant, which used pulverized coal.

2.3.1. Case Study 1: Fuel and λ Variation

In this context, the objective was to examine the fundamental characteristics of the base situation, specifically the combustion of coal. As an alternative to this fuel source, we tested methane (for comparison with the most-used fuel in power plants in Portugal) and pine sawdust (as a replacement for coal). The combustion parameters for each fuel ranged between $\lambda = 1$ to $\lambda = 2.2$, using the operating conditions in Table 1, with a reheating pressure of 3.1 bar.

The properties of the tested biomass were obtained from the literature [34]. The biomass studied resulted from forest cleaning operations, undertaken to reduce the risk of fire. It is a product with low economic value and therefore represents an ideal fuel for the transfer of heat.

2.3.2. Case Study 2: Variation in Reheating Pressure and λ

In this scenario, the reheating pressure was studied to verify its impact on the adiabatic flame temperature and emissions of CO₂ due to excess air. A range of reheating pressures between half to one-eighth of the operating pressure, as well as the typical optimal condition, were tested (one-quarter of the operating pressure) [24]. This scenario was simulated for methane, coal, and biomass.

2.3.3. Case Study 3: Coal and Biomass Co-Combustion

This scenario simulated the co-combustion of coal and biomass. The following combinations were tested: 25% coal–75% biomass; 50% coal–50% biomass and; 75% coal–25% biomass. In all tested situations, the adiabatic flame temperature and carbon dioxide emission (CO₂) were analyzed according to the excess air.

3. Simulation Results

3.1. Case Study 1: Fuel and λ Variation

A total of five combustion conditions were tested, spanning a range of λ values from 1 to 2.2 for methane, coal, and pine sawdust. The steam generator operation pressure was set at 12.5 bar, with a reheating pressure of 3.1 bar (approximately one-quarter of the operation pressure). Figure 2 presents the reduction in the temperature of flue gas as it exchanges heat with the various components of the water–steam circuit.

It was observed that methane and coal provide similar flame temperatures (although 2 to 4% lower with coal with increasing λ). Pine sawdust generates adiabatic flame temperatures that are 18 to 15% lower than those of methane and coal with increasing λ . This difference in adiabatic flame temperatures determines the maximum operation λ , which is necessary to enable heat exchange in the economizer. To maintain the flue gas temperature higher than the water economizer inlet temperature, methane was limited to $\lambda \leq 2.2$, coal to $\lambda \leq 1.9$ and pine sawdust to $\lambda \leq 1.6$.

Table 3 presents the CO₂ mass flow emission and concentration based on the molar balance. The concentration was calculated on a dry basis for the corresponding oxygen concentration and corrected to 3% O₂ to compare the simulation results.

As evidenced in Table 3, solid fuel produces a greater CO₂ mass emission due to its lower LHV and higher carbon content. Among the solid fuels, pine sawdust emits 14% more CO₂ in mass but a similar concentration, corrected to 3% O₂. However, it should be noted that biomass is a carbon-neutral energy source.

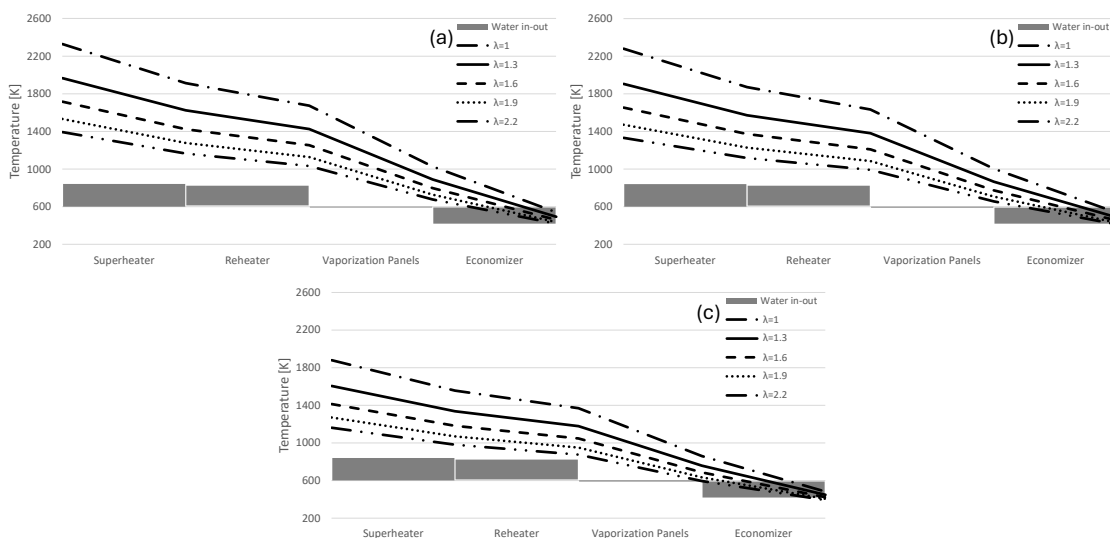


Figure 2. Water–steam inlet and outlet temperatures of heat exchangers and flue gas temperatures for several λ conditions: (a) methane; (b) coal; (c) pine sawdust.

Table 3. CO₂ emissions for methane, coal, and pine sawdust.

	CO ₂ [kg/s]	[CO ₂] @ Minimum λ	[CO ₂] @ 3% O ₂
Methane	32.24	5.01 ($\lambda = 2.2$)	10.12
Coal	61.10	9.75 ($\lambda = 1.9$)	16.14
Pine sawdust	69.66	11.41 ($\lambda = 1.6$)	15.87

3.2. Case Study 2: Reheating Pressure and Excess Air

The effects of water–steam reheating pressure on CO₂ emissions were examined for the three fuels. In this study, it was assumed that all the inlet and outlet temperatures of the economizer, vaporization panels, and superheater remained constant at the operating pressure of 12.5 bar. This was chosen to align with the operational conditions of the power plant and to ensure that the materials used would remain within their metallurgical limits. Furthermore, the reheater outlet temperature was also maintained. Since this is a preliminary study regarding the retrofitting of existing coal-fired power plants, it should be noted that this study did not analyze the impacts of the reheating pressure in the steam turbines and remaining components of the power plant. The remaining equipment will be addressed in further iterations of the developed numerical tool.

Figure 3 presents the impact of changing the reheating pressure on the CO₂ emissions for the three fuels tested.

As illustrated in Figure 3, an increase in reheating pressure reduces CO₂ emissions, regardless of the fuel used. It can thus be postulated that modifying the reheating conditions may prove to be an effective method for reducing CO₂ mass flow emissions by up to 7%. However, the consequences of modifying the reheat pressure were not considered with respect to steam turbine and condenser operation or regarding overall efficiency.

Furthermore, the influence of fuel type on CO₂ emissions is more pronounced than modifying the reheat pressure: 14% higher for biomass compared with coal, and 89% higher for coal compared with methane. Accordingly, the typical operation pressure of 3.1 bar (one-quarter of the operating pressure) was employed as a reference point, given that the potential CO₂ variation with reheating pressure is only between 5.5% (one-eighth of the operating pressure) and –6.9% for one-half of the operating pressure.

Furthermore, since biomass is carbon-neutral, reheat pressure has a negligible impact. Due to the low LHV of biomass, it is commonly mixed with coal to provide a higher adiabatic flame temperature, thereby improving the heat exchange transfer while reducing the environmental impact.

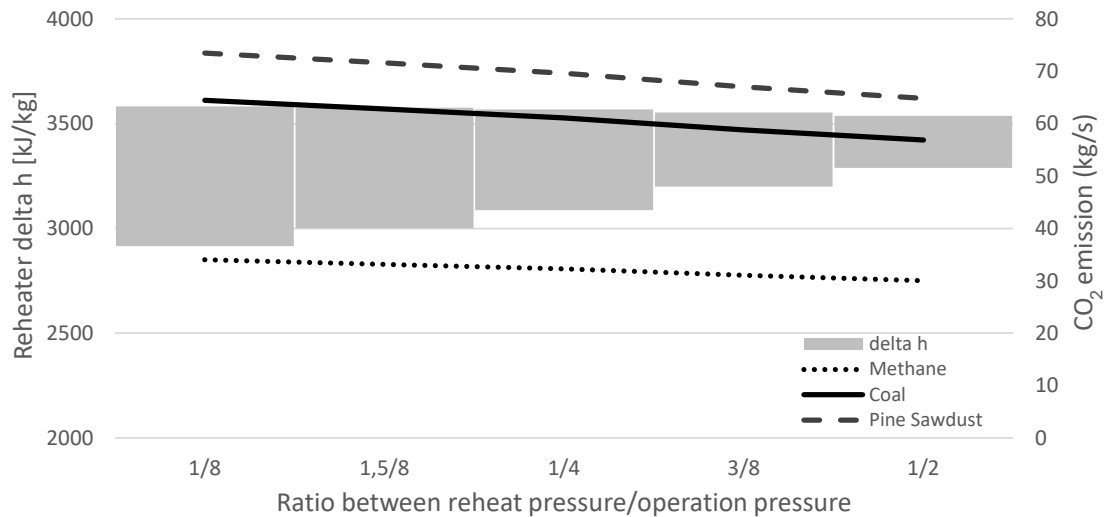


Figure 3. Water–steam inlet and outlet enthalpies of heat exchangers and CO₂ mass flow emissions ($\lambda = 1.3$) for methane, coal, and pine sawdust.

3.3. Case Study 3: Coal and Biomass Co-Combustion

The co-combustion of coal and biomass was examined to ascertain the CO₂ mass flow emissions and the combustion conditions necessary to meet the operational conditions of the power plant. These conditions included the inlet and outlet temperatures of the economizer, vaporization panels, and superheater, which are constant at operating pressures of 12.5 bar and 3.1 bar of reheating pressure. Figure 4 presents the adiabatic flame temperatures and CO₂ mass flow emissions for several co-combustion mixtures of coal and pine sawdust.

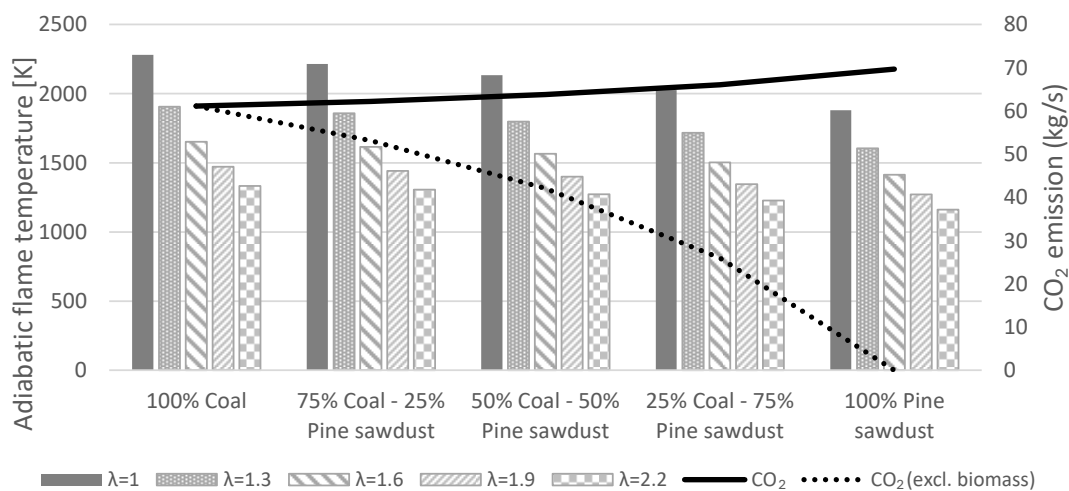


Figure 4. Adiabatic flame temperature and CO₂ mass flow emissions for coal and pine sawdust combinations.

Figure 4 shows that the co-combustion of coal and pine sawdust has a beneficial impact on adiabatic flame temperature, even when 25% coal–75% pine sawdust (molar percentages) is employed. Using coal as reference, the adiabatic flame temperature declines, on average, by 2.3%, 5.3%, and 9.3% with the incremental incorporation of pine sawdust, ranging from 25%, 50% and 75%, respectively. The use of 100% pine sawdust results in an average reduction of 14.8%.

To maintain the power plant’s \dot{W}_{useful} , increasing the percentage of pine sawdust results in an increase of up to 14% in CO₂ mass emissions when using 100% biomass in

comparison to coal. This is due to the lower *LHV* of pine sawdust compared with that of coal. However, as the CO₂ emissions from renewable sources were not considered, increasing biomass leads to reductions of 13% (25% biomass), 31% (50% biomass), and 57% (75% biomass) compared to 100% coal. This suggests that pine sawdust can be used as a replacement for coal, even at higher percentages.

Figure 5 presents the operational impacts on the economizer regarding exhaust gas outlet and water inlet temperature, as well as the CO₂ concentration, resulting from using different λ values.

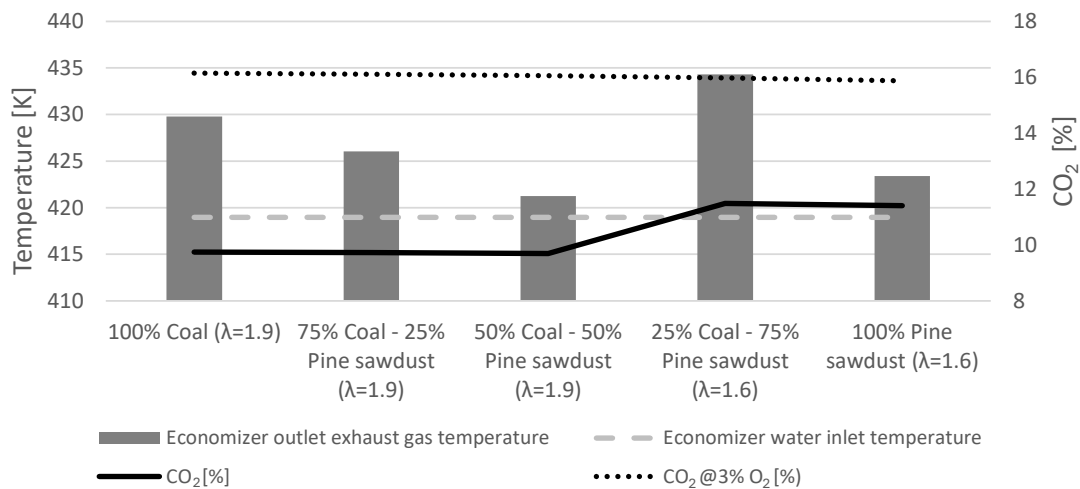


Figure 5. Economizer outlet exhaust gas temperature for minimum λ , economizer water inlet temperature and CO₂ concentration.

For heat exchange to occur, the temperature of the exhaust gas temperature at the economizer outlet must exceed that of the economizer water inlet. It is possible to operate at $\lambda = 1.9$ with a mixture of up to 50% coal–50% pine sawdust, which provides a high CO₂ dilution (9.7% concentration). Upon correcting all samples to 3% O₂ concentration, no significant differences were observed.

For a fuel blend of 25% coal and 75% pine sawdust, it was possible to operate at $\lambda = 1.8$, although only $\lambda = 1.6$ is shown for reasons of coherence with previous results. This demonstrates that a small amount of coal contributes positively to maintaining the power plant's operation near the coal combustion parameters, with a reduction of 57.5% in CO₂ emissions (considering the biomass as carbon-neutral).

4. Conclusions

Reaching the European Union goals of decarbonization via an expected transition to electricity requires an increase amount of electric energy production. During the recent shortage of natural gas, it was necessary to promote the diversification of electricity sources, restarting the public debate on the phasing out of coal-fired power plants. For instance, in Germany, this debate led to the restarting of coal-fired power plants despite the CO₂ production and decarbonization plans. Additionally, the needs to reduce the country's energy dependence and meet peak demands represent an opportunity to retrofit current coal-fired power plants to operate with 100% biomass or use the co-combustion of coal and biomass. This offers advantages for reducing CO₂ emissions, with biomass potentially being considered carbon-neutral in emission accounting. This paper considered the Sines power plant as a case study, which is located in Portugal; however, the solution presented can be applied to similar power plants with pulverized solid fuel burners.

Although coal can use higher λ , a mixture of coal and biomass can operate between 1.9 and 1.6, maintaining the operational conditions of the considered Sines power plant. Moreover, a fuel blend composed of 25% coal and 75% pine sawdust allows operation at $\lambda = 1.8$, demonstrating that a small amount of coal allows operation near the coal combus-

tion parameters, with a reduction of 57.5% in CO₂ emissions (considering the biomass as carbon-neutral).

The introduction of biomass reduces the adiabatic flame temperature, on average, by between 2.3% ± 0.3%, 5.3% ± 0.7%, and 9.3% ± 1.2% with the incremental incorporation of pine sawdust, up to 14.8% ± 1.8% when 100% pine sawdust is used. Nonetheless, even for 25% coal and 75% pine sawdust, an 8.7% reduction in T_{ad} still allows operation at $\lambda = 1.8$, which is very close to that of coal ($\lambda = 1.9$).

Future applications of the developed tool include the use of hydrogen to improve the biomass combustion parameters, namely, to increase the adiabatic flame temperature, allowing the reduction in or the elimination of the need to use coal. This will also contribute to decarbonization strategies and to the diversification of the fuels used for electricity production, reducing the country's dependency on energy sources.

Author Contributions: Conceptualization, C.S.S.L.C.; methodology, P.B., F.C., G.O.D. and C.S.S.L.C.; validation, G.O.D.; formal analysis, F.C.; investigation, V.B.; data curation, V.B.; writing—original draft preparation, G.O.D. and C.S.S.L.C.; writing—review and editing, P.B., F.C. and C.S.S.L.C.; supervision, C.S.S.L.C.; project administration, C.S.S.L.C. All authors have read and agreed to the published version of the manuscript.

Funding: This research was funded by Polytechnic University of Lisbon grant number IPL/IDI&CA2023/GEErVap_ISEL.

Institutional Review Board Statement: Not applicable.

Informed Consent Statement: Not applicable.

Data Availability Statement: The data in the paper belong to the authors and are not for public use. They can be made available upon request.

Acknowledgments: P. Baptista and G. O. Duarte acknowledge support from the Fundação para a Ciência e Tecnologia through project UIDB/50009/2020—IST-ID.

Conflicts of Interest: The authors declare no conflict of interest.

References

1. European Commission. *Communication from the Commission to the European Parliament, the European Council, the Council, the European Economic and Social Committee and the Committee of the Regions: A Green Deal Industrial Plan for the Net-Zero Age*; European Commission: Brussels, Belgium, 2023.
2. Jacobson, M.Z. Roadmaps to Transition Countries to 100% Clean, Renewable Energy for All Purposes to Curtail Global Warming, Air Pollution, and Energy Risk. *Earth's Futur.* **2017**, *5*, 948–952. [CrossRef]
3. International Energy Agency. Net Zero by 2050: A Roadmap for the Global Energy Sector. 2021. Available online: https://iea.blob.core.windows.net/assets/deebef5d-0c34-4539-9d0c-10b13d840027/NetZeroby2050-ARoadmapfortheGlobalEnergySector_CORR.pdf (accessed on 14 July 2024).
4. República Portuguesa. Plano Nacional de Energia e Clima 2021–2030 (PNEC 2030). 2018. Available online: <https://apambiente.pt/clima/plano-nacional-de-energia-e-clima-pnec> (accessed on 14 July 2024).
5. República Portuguesa, Fundo Ambiental, and Portuguese Environment Agency. Roadmap for Carbon Neutrality 2050 (RNC2050). 2019. Available online: https://unfccc.int/sites/default/files/resource/RNC2050_EN_PT%20Long%20Term%20Strategy.pdf (accessed on 14 July 2024).
6. Felício, L.; Henriques, S.T.; Guevara, Z.; Sousa, T. From electrification to decarbonization: Insights from Portugal's experience (1960–2016). *Renew. Sustain. Energy Rev.* **2024**, *198*, 114419. [CrossRef]
7. Portuguese Environment Agency. Roteiro Nacional de Baixo Carbono 2050; 2012. Available online: <https://apambiente.pt/clima/roteiro-nacional-de-baixo-carbono-2050> (accessed on 14 July 2024).
8. DGEG—Direção Geral de Energia e Geologia. Balanço Energético Nacional 2021. Lisboa, 2022. Available online: <https://www.dgeg.gov.pt/media/kmoflag/dgeg-ben-2021.pdf> (accessed on 14 July 2024).
9. Ferreira, P.T.; Fernandes, U.; Casaca, C.; Ferreira, M.E.C.; Teixeira, J.C.F.; Costa, M. Particulate matter emissions and fly ash characteristics in a pulverized biomass fired large-scale laboratory furnace. In Proceedings of the 12th International Conference on Energy for a Clean Environment, Lisboa, Portugal, 5–9 July 2015.
10. Zhu, Z.; Zhao, J.; Liu, Y. The impact of energy imports on green innovation in the context of the Russia-Ukraine war. *J. Environ. Manag.* **2024**, *349*, 119591. [CrossRef] [PubMed]
11. Eurostat. Database-Eurostat. Available online: <https://ec.europa.eu/eurostat/web/main/data/database> (accessed on 14 July 2024).

12. Eurostat. Database-Eurostat. Available online: <https://ec.europa.eu/eurostat/web/energy/database> (accessed on 14 July 2024).
13. Zhang, Y.-L.; Liu, L.-C.; Kang, J.-N.; Peng, S.; Mi, Z.; Liao, H.; Wei, Y.-M. Economic feasibility assessment of coal-biomass co-firing power generation technology. *Energy* **2024**, *296*, 131092. [[CrossRef](#)]
14. Al-Mansour, F.; Zuwala, J. An evaluation of biomass co-firing in Europe. *Biomass-Bioenergy* **2010**, *34*, 620–629. [[CrossRef](#)]
15. Liu, L.; Memon, M.Z.; Xie, Y.; Gao, S.; Guo, Y.; Dong, J.; Gao, Y.; Li, A.; Ji, G. Recent advances of research in coal and biomass co-firing for electricity and heat generation. *Circ. Econ.* **2023**, *2*, 100063. [[CrossRef](#)]
16. Balmer, R.T. *Modern Engineering Thermodynamics*; Elsevier: Amsterdam, The Netherlands, 2011. [[CrossRef](#)]
17. Aviso, K.; Sy, C.; Tan, R.; Ubando, A. Fuzzy optimization of carbon management networks based on direct and indirect biomass co-firing. *Renew. Sustain. Energy Rev.* **2020**, *132*, 110035. [[CrossRef](#)]
18. Xu, J.; Huang, Q.; Lv, C.; Feng, Q.; Wang, F. Carbon emissions reductions oriented dynamic equilibrium strategy using biomass-coal co-firing. *Energy Policy* **2018**, *123*, 184–197. [[CrossRef](#)]
19. Juanico, F.J.M. *Geradores de Calor*; Ecemei: Porto, Portugal, 1992.
20. Annaratone, D. *Steam Generators Description and Design*; Springer: Berlin/Heidelberg, Germany, 2008.
21. Kakaç, S. *Boilers, Evaporators, and Condensers*; Wiley: Hoboken, NJ, USA, 1991.
22. Ahmed, A.; Esmaeil, K.K.; Irfan, M.A.; Al-Mufadi, F.A. Design methodology of heat recovery steam generator in electric utility for waste heat recovery. *Int. J. Low-Carbon Technol.* **2018**, *13*, 369–379. [[CrossRef](#)]
23. Bhogade, D.S. Ultra supercritical thermal power plant material advancements: A review. *J. Alloy. Met. Syst.* **2023**, *3*, 100024. [[CrossRef](#)]
24. Opreiș, I.; Cenușă, V.-E.; Norișor, M.; Darie, G.; Alexe, F.-N.; Costinaș, S. Parametric optimization of the thermodynamic cycle design for supercritical steam power plants. *Energy Convers. Manag.* **2020**, *208*, 112587. [[CrossRef](#)]
25. Wang, Y.; Li, X.; Mao, T.; Hu, P.; Li, X.; Wang, G. Mechanism modeling of optimal excess air coefficient for operating in coal fired boiler. *Energy* **2022**, *261*, 125128. [[CrossRef](#)]
26. Pedro, C.; Costa, M. Combustão. In *Edições Orion*. 2007. Available online: <https://scholar.tecnico.ulisboa.pt/records/5d807c7f-ff9d-4f8e-b5ad-0a20e370d3d2?lang=pt> (accessed on 14 July 2024).
27. Glavan, I.; Poljak, I.; Kosor, M. A gas turbine combustion chamber modeling by physical model. *Pomorstvo* **2021**, *35*, 30–35. [[CrossRef](#)]
28. Yu, Z.; Ma, X.; Liao, Y. Mathematical modeling of combustion in a grate-fired boiler burning straw and effect of operating conditions under air- and oxygen-enriched atmospheres. *Renew. Energy* **2010**, *35*, 895–903. [[CrossRef](#)]
29. Elorf, A.; Sarh, B. Excess air ratio effects on flow and combustion characteristics of pulverized biomass (olive cake). *Case Stud. Therm. Eng.* **2019**, *13*, 100367. [[CrossRef](#)]
30. Houshfar, E.; Skreiberg, Ø.; Løvås, T.; Todorović, D.; Sørnum, L. Effect of Excess Air Ratio and Temperature on NO_x Emission from Grate Combustion of Biomass in the Staged Air Combustion Scenario. *Energy Fuels* **2011**, *25*, 4643–4654. [[CrossRef](#)]
31. Zhang, G. Study on Optimum Excess Air Coefficient for Power Plant Boilers. In Proceedings of the 2015 International Conference on Mechatronics, Electronic, Industrial and Control Engineering, Shenyang, China, 1–3 April 2015; Atlantis Press: Paris, France, 2015. [[CrossRef](#)]
32. Zeng, W.; Pang, L.; Zheng, W.; Hu, E. Study on combustion and emission characteristics of a heavy-duty gas turbine combustor fueled with natural gas. *Fuel* **2020**, *275*, 117988. [[CrossRef](#)]
33. Ji, Y.; Zhang, S.; Wang, K.; Qi, G. Study on combustion and nitrogen oxide emissions of gas boiler. *IOP Conf. Ser. Mater. Sci. Eng.* **2020**, *721*, 012054. [[CrossRef](#)]
34. Casaca, C.; Costa, M. Co-combustion of biomass in a natural gas-fired furnace. *Combust. Sci. Technol.* **2003**, *175*, 1953–1977. [[CrossRef](#)]

Disclaimer/Publisher’s Note: The statements, opinions and data contained in all publications are solely those of the individual author(s) and contributor(s) and not of MDPI and/or the editor(s). MDPI and/or the editor(s) disclaim responsibility for any injury to people or property resulting from any ideas, methods, instructions or products referred to in the content.